Pressure-Induced Superconductivity in Noncentrosymmetric Heavy-Fermion CeRhSi$_3$

N. Kimura, K. Ito, K. Saitoh, Y. Umeda, and H. Aoki

Center for Low Temperature Science, Tohoku University, Sendai, Miyagi 980-8578, Japan

T. Terashima

National Institute for Materials Science, Tsukuba, Ibaraki 305-0047, Japan

We report the pressure-induced superconductivity in the noncentrosymmetric heavy-fermion CeRhSi$_3$. The superconductivity emerges above about 12 kbar even though the antiferromagnetic ordering persists. Furthermore, another anomaly is observed in the superconducting phase. The anomalous magnetic field-temperature phase diagram with a high upper critical field suggests that an unconventional superconductivity is realized in CeRhSi$_3$.

Several Ce-based heavy-fermion materials have been found to exhibit superconductivity (SC) near the quantum critical point where magnetic ordering is suppressed [1–5]. Magnetic fluctuation is the most presumable candidate for the attractive interaction of the Cooper pair in this SC. A consensus has been established that non-s-wave pairing is favorable for such a magnetically mediated superconductor (MMSC). In centrosymmetric materials, to which most superconductors belong, spin and orbital parts of the pair function can be treated individually since conduction bands are degenerate even if the spin-orbit coupling (SOC) is strong. Therefore, we can express the Cooper pair as, for example, a spin-singlet s wave or a spin-triplet p wave.

The newly discovered SC in heavy-fermion CePt$_3$Si [6] and itinerant ferromagnet UIr [7] requires a modification of the established description of the pair function since these materials do not possess an inversion center. In a non-centrosymmetric material, the spin-orbit interaction lifts the degeneracy of the conduction bands; therefore, we can no longer treat the spin and orbital parts of pair function independently [8,9]. In this situation, the SOC is expected to play an important role for formation of a new class of the pair function, especially in the MMSC. A search for other noncentrosymmetric superconductors is thus important for understanding the mechanism of the MMSC as well as for verification of new theoretical works motivated by the discovery of CePt$_3$Si [10–12]. In this Letter, a new example of a pressure-induced SC in noncentrosymmetric heavy-fermion CeRhSi$_3$ is presented. Furthermore, the resistivity and ac-susceptibility measurements demonstrate an anomalous superconducting phase diagram, indicating that an unconventional SC is realized in this material.

The crystal structure of CeRhSi$_3$ is BaNiSn$_3$-type belonging to space group $I4mm$ (No. 107) without an inversion center [13] as shown in the inset in Fig. 1(b). CeRhSi$_3$ exhibits the antiferromagnetic (AFM) ordering below $T_N = 1.6$ K. The antiferromagnetism is robust against the magnetic field probably due to a strong Kondo screening effect on the $4f$ electron. The electronic specific heat coefficient γ is about 120 mJ/mol K^2 [13]. The de Haas–

van Alphen (dHvA) experiment reveals heavy quasiparticles and that their bands finely split due to the spin-orbit interaction, which is characteristic of the noncentrosymmetric material [14].
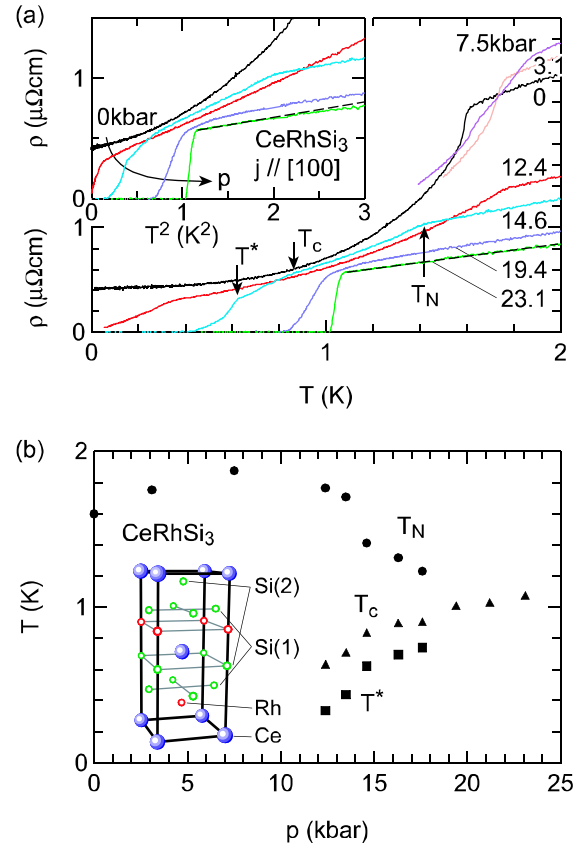
FIG. 1 (color online).   (a) Electrical resistivity as a function of temperature for several pressures from ambient pressure (0 kbar) to 23.1 kbar. T^2 dependences are plotted for the corresponding pressures except for the traces at 3.1 and 7.5 kbar in the inset. For the 23.1 kbar data, the broken lines show T-linear (main panel) and T^2 (inset) dependence. (b) Illustration of the crystal structure and temperature-pressure phase diagram of CeRhSi$_3$ based on resistivity measurements.

P H Y S I C A L   R E V I E W   L E T T E R S

Single crystals of CeRhSi$_3$ were grown by the Czochralski pulling method in a tetra-arc furnace under Ar gas atmosphere. Starting materials were 4N (99.99% pure)-Ce, 3N-Rh, and 5N-Si. The resultant ingots of the single crystals were annealed at 900 °C under a vacuum of 2×10^{-6} torr for a week. Two samples were cut from different ingots; one was used for resistivity measurements and the other mostly for ac-susceptibility measurements. The residual resistivity ρ_0 and its ratio (RRR) for the resistivity sample with a current along the [100] direction were 0.42 $\mu\Omega$ cm and 180, respectively. The ac-susceptibility sample also has a RRR larger than 100. The qualities of these samples are better than that of the previous sample for the dHvA experiment [14], which has a RRR of 64 and a mean free path of $l \approx 2000$ Å. Hydrostatic pressures up to 23.1 kbar were produced by clamped piston cylinder cells. The same setup was successfully used for the dHvA experiments under pressure, indicating that hydrostatic pressures of high quality can be applied [15]. The pressures at low temperatures were determined by the resistivity of manganin wire which was calibrated against the ac-susceptibility drop of the superconducting transition of Sn. The resistivity was measured by a low-frequency ac four-terminal method with current $j = 0.136$ A/cm^2. The pick-up coil for the ac-susceptibility measurement was calibrated by the superconductive shielding of Sn whose dimension is the same as the present sample. The frequency and the amplitude of excitation field were 138 Hz and 0.01–0.1 Oe, respectively.

Figure 1(a) shows the pressure dependence of the resistivity as a function of temperature. The T_N (=1.6 K at 0 kbar) initially increases with increasing pressure, and then it turns to decrease above 7.5 kbar and the resistivity drop at T_N becomes less obvious. Above about 20 kbar, T_N becomes difficult to determine.

For $p \gtrsim 12.4$ kbar, another rapid decrease of resistivity appears at a lower temperature. The resistivity decrease becomes sharper at higher pressures. Since the resistivity decreases to zero, it is very likely that the SC emerges at high pressures. We denote the onset temperature of the resistivity decrease as T_c. At some pressures like 14.6 kbar, an additional rapid decrease of resistivity is noted below T_c. The temperature is denoted by T^* and plotted in Fig. 1(b) together with T_N and T_c as a function of pressure. It is interesting to note that T_c and T^* exhibit similar p dependence. T^* becomes difficult to identify at high pressures because the resistivity drops sharply at T_c. The anomaly at T^* will be further described later. Figures 1(a) and 1(b) clearly indicate that the superconductivity emerges in the AFM phase.

The inset in Fig. 1(a) shows the resistivity plotted against T^2. The temperature dependence of the resistivity at 0 kbar demonstrates the Fermi liquid behavior, namely, $\rho = \rho_0 + AT^2$, below 0.6 K with the coefficient $A \approx$ 0.2 $\mu\Omega$ cm/K^2. The resistivities at pressures from 12.4 to 17.6 kbar are well fitted by T^2 power law below T_N. The coefficient A is enhanced to be 0.32–0.35 $\mu\Omega$ cm/K^2 at these pressures, indicating that the value of γ is enhanced under pressure. The temperature dependence changes from 19.4 kbar where the antiferromagnetism appears to vanish. Comparing the data for 23.1 kbar with the broken straight lines in the main and inset panels, we see that the T-linear dependence at 23.1 kbar is better described by T linear (main panel) than T^2 (inset). This reminds us of the fact that the T^2 behavior of the resistivity in CePt$_3$Si changes to T^1 at about 6 kbar, where T_N vanishes [16].

To verify whether the bulk SC is realized in CeRhSi$_3$, we have carried out the ac-susceptibility measurements at 16.2 kbar. Figure 2(a) shows the real and imaginary parts of the susceptibility χ' and χ'' as a function of temperature. Since the excitation field was much reduced to see the SC transition, the AFM transition is not obviously detected in the present measurement and is not shown in the figure. With decreasing temperature, χ' starts to decrease from about 0.87 K, then decreases rapidly from about 0.4 K, and finally reaches the value of $4\pi\chi' = -1$ at lowest tempera-
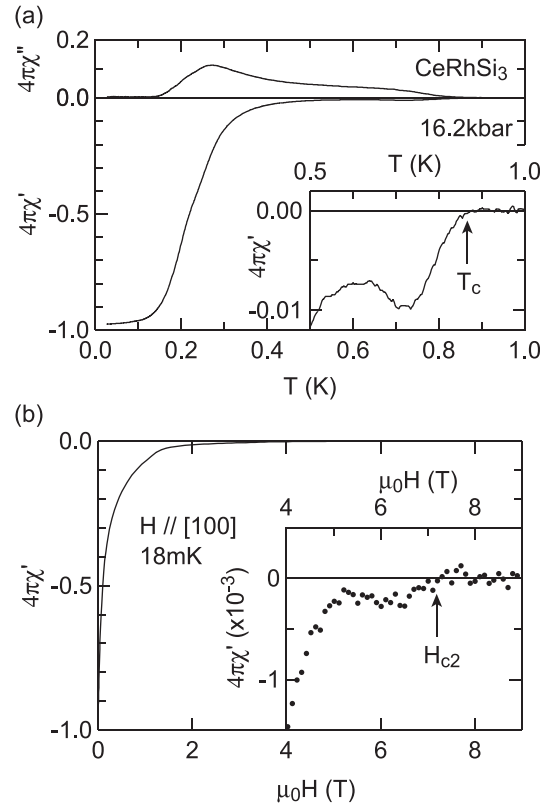
FIG. 2. (a) Zero-field ac susceptibility as a function of temperature at 16.2 kbar. An enlarged view of χ' above 0.5 K is shown in the inset. The excitation field amplitude is 0.01 Oe. (b) Base-temperature susceptibility as a function of field for field along the [100] direction. An enlarged view of χ' above 4 T is shown in the inset. The excitation field amplitude is 0.1 Oe. The normal state contribution is subtracted.

tures. The onset temperature of the shielding approximately corresponds to T_c defined by the resistivity measurement. Since zero resistivity is attained at a much lower temperature, the T_c determined by the ac susceptibility can be assumed to be the onset temperature of bulk SC. On the other hand, χ'' has a peak around the temperatures where χ' decreases rapidly as is usually observed in a superconductor.

As shown in the inset in Fig. 2(a), χ' shows a minimum at about 0.72 K. Accordingly, a sizable amplitude of χ'' extends to higher temperatures, making a shoulderlike structure around the same temperature. The origin of these anomalies is unclear, but it might be associated with the anomaly at T^* in the resistivity.

Figure 2(b) shows the susceptibility as a function of magnetic field at 18 mK. χ' increases rapidly with application of small magnetic fields but then continues to increase gradually with field. We denote the field where the paramagnetic value is recovered as the upper critical field H_{c2}, which is as high as 7 T. As shown in the inset, in addition to the change at H_{c2}, there seems to be another small change in χ' around 6 T. A minimum of the χ', similar to that in the inset in Fig. 2(a), is also observed in the temperature sweep at 6 T.

To elucidate the nature of the anomalies observed in the resistivity and susceptibility measurements, we have investigated the resistivity under magnetic fields at several pressures. We show the temperature dependence of the resistivity at 14.6 kbar for various fields in Fig. 3. Two resistivity drops can be clearly observed at zero magnetic field. The resistivity below T_c diminishes considerably with decreasing current, while the anomaly at T^* takes place at nearly the same temperature for the two current densities. With application of magnetic field, the resistivity drop at T_c becomes less obvious, while the one at T^*

broadens under low fields, and then it becomes sharper again at higher fields above 1 T. Similar behavior is observed at 19.4 kbar. Although T^* is absent at 0 T, T^* appears in fields and the associated resistivity drop sharpens at high fields. At 23.1 kbar, no obvious anomaly appears in the resistivity curve below T_c.

In Fig. 4, we plot the temperatures T_N, T_c, and T^* and fields H_{c2} determined from the resistivity measurements at 14.6 kbar and the ac-susceptibility measurements at 16.2 kbar as the H-T phase diagram. T_N is still robust against the magnetic field even at 14.6 kbar. The boundary between normal and superconducting states, namely, the H_{c2} curve, has an unusual shape. It seems to follow initially a normal BCS-like curve but subsequently increases steeply below 0.3 K.

At 16.2 kbar, the upper critical field $H_{c2}(0)$ for $T \rightarrow 0$ reaches 7 T, largely exceeding the Pauli-Clogston limiting field given by $H_P \approx 1.86$ [T/K] $\times T_c$[K] [17]. From the well-known formula $\mu_0 H_{c2}(0) = \Phi_0/(2\pi\xi_0^2)$, the coherence length ξ_0 is estimated to be 70 Å, which indicates that the present sample, where l is expected to exceed 2000 Å, is in the clean limit. The initial slope of $H_{c2}(T)$ is given by the broken line in Fig. 4 and has the value $(dH_{c2}/dT_c)|_{T_c} \approx -12$ T/K. Considering the enhanced value of γ under pressure, these values can be compared to $H_{c2} = 5$ T, $dH_{c2}/dT_c = -8$ T/K of CePt$_3$Si with γ of 390 mJ/mol K^2 [6]. The phase diagram of CeRhSi$_3$ is entirely different from that of the reference material of LaRhSi$_3$ with $T_c = 1.9$ K and $H_c = 0.03$ T. The high upper critical field also indicates that the SC of CeRhSi$_3$ is unconventional.

Moreover, it appears from the plot of T^* that there is another boundary inside the H_{c2} curve. Two superconduct-

FIG. 3 (color online).   Electrical resistivity as a function of temperature for several fields at 14.6 kbar. Magnetic fields are applied along the [100] direction. T^2 fitting curves are also plotted by dotted lines. T_c and T^* are indicated by arrows. All the data were measured for a current $j = 0.136$ A/cm^2, except for the second trace at 0 T, which is for $j = 0.034$ A/cm^2.
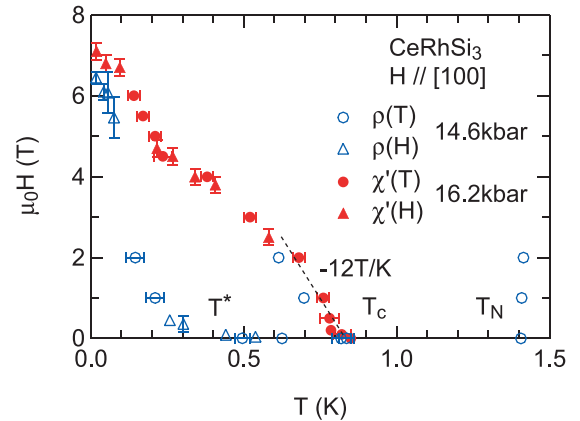
FIG. 4 (color online).   Magnetic field-temperature phase diagram of CeRhSi$_3$ constructed from resistivity at 14.6 kbar and ac-susceptibility measurements at 16.2 kbar. Solid circles and triangles denote the transition temperatures and fields determined by $\chi'(T)$ and $\chi'(H)$, respectively. Hollow circles and triangles denote those determined by $\rho(T)$ and $\rho(H)$, respectively. The initial slope $(dH_{c2}/dT_c)|_{T_c}$ is indicated by a broken line.

ing phases which are spatially separated and have different superconducting properties could give rise to such a phase diagram in Fig. 4. However, if the second SC emerges in other places than those of the first SC, the susceptibility is expected to decrease further upon the occurrence of the second SC with lower T_c and H_{c2}. The observations of the susceptibilities at 0.72 K in Fig. 2(a) is inconsistent with this prediction. Furthermore, an intergrain or percolated-impurity effect is not expected for the present high quality single crystals and for experiments under hydrostatic pressures of high homogeneity. The existence of the anomaly below T_c and broadened transition in the resistivity have been reported also in high quality $CePt_3Si$ under pressure [16]. In these respects, the superconducting properties of $CeRhSi_3$ are similar to those of $CePt_3Si$.

Among the superconductors so far investigated, heavy-fermion superconductor UPt_3 and the rare-earth (RE) magnetic superconductors of the $(RE)Mo_6X_8$ type ($X = $ S, Se) and $(RE)Rh_4B_4$ type appear to have similar features. In the former compound, the multiple superconducting phases and a double structure in ac susceptibility are observed [18]. However, the superconducting drop of the resistivity is sharp and takes place only at the higher T_c. The behavior of $CeRhSi_3$ below 20 kbar is different from these behaviors. On the other hand, in the latter compounds, the shape of the phase boundary is similar to the characteristic shape of the boundaries in $CeRhSi_3$, which is concave around 0.3 K, and similar features of susceptibility to those in Fig. 2(a) are also observed [19]. The resemblances might suggest that the anomaly at T^* in $CeRhSi_3$ is related to a change of magnetism. This scenario is consistent with the vanishing of T^* at the pressure where the AFM transition disappears. However, it is not clear why T^* can be observed in χ despite the fact that T_N itself cannot be detected and why T_c and T^* exhibit similar p dependence. Microscopic measurements would be necessary to reveal the origin of the anomalous phase diagram of $CeRhSi_3$.

In summary, $CeRhSi_3$ is found to be a new member of the pressure-induced noncentrosymmetric heavy-fermion superconductor. The SC exists even in the AFM state. Another anomaly emerges in the superconducting phase. The high upper critical field and the anomalous phase diagram indicate that the SC is unconventional.

[1] N. D. Mathur et al., Nature (London) **394**, 39 (1998).
[2] E. Vargoz, and D. Jaccard, J. Magn. Magn. Mater. **177**, 294 (1998).
[3] T. C. Kobayashi et al., J. Phys. Soc. Jpn. **67**, 996 (1998).
[4] R. Movshovich et al., Phys. Rev. B **53**, 8241 (1996).
[5] H. Hegger et al., Phys. Rev. Lett. **84**, 4986 (2000).
[6] E. Bauer et al., Phys. Rev. Lett. **92**, 027003 (2004).
[7] T. Akazawa et al., J. Phys. Condens. Matter **16**, L29 (2004).
[8] L. P. Gor'kov and E. I. Rashba, Phys. Rev. Lett. **87**, 037004 (2001).
[9] S. S. Saxena and P. Monthoux, Nature (London) **427**, 799 (2004).
[10] K. V. Samokhin, E. S. Zijlstra, and S. K. Bose, Phys. Rev. B **69**, 094514 (2004).
[11] P. A. Frigeri, D. F. Agterberg, A. Koga, and M. Sigrist, Phys. Rev. Lett. **92**, 097001 (2004).
[12] H. Shimahara, J. Phys. Soc. Jpn. **73**, 2635 (2004).
[13] Y. Muro et al., J. Phys. Soc. Jpn. **67**, 3601 (1998).
[14] N. Kimura et al., Physica (Amsterdam) **294B–295B**, 280 (2001).
[15] M. Endo et al., Phys. Rev. Lett. **93**, 247003 (2004).
[16] T. Yasuda et al., J. Phys. Soc. Jpn. **73**, 1657 (2004).
[17] A. M. Clogston, Phys. Rev. Lett. **9**, 266 (1962).
[18] Z. Kozioł et al., Physica (Amsterdam) **192C**, 284 (1992).
[19] See, e.g., *Superconductivity in Ternary Compounds II*, edited by M. B. Maple and Ø. Fischer (Springer-Verlag, Berlin, 1982).